Microchemical Journal 131 (2017) 57–69

Contents lists available at ScienceDirect

Microchemical Journal

journal homepage: www.elsevier.com/locate/microc

On-line micro-solid phase preconcentration of Cd^{2+} coupled to TS-FF-AAS using a novel ion-selective bifunctional hybrid imprinted adsorbent

César Ricardo Teixeira Tarley [a,c,*], Marcela Zanetti Corazza [a], Fernanda Midori de Oliveira [a], Bruna Fabrin Somera [a], Clésia Cristina Nascentes [b], Mariana Gava Segatelli [a]

[a] Departamento de Química, Universidade Estadual de Londrina (UEL), Rod. Celso Garcia Cid, PR 445 Km 380, Campus Universitário, Londrina, PR CEP 86051-990, Brazil
[b] Departamento de Química, Instituto de Ciências Exatas, Universidade Federal de Minas Gerais (UFMG), Av. Antonio Carlos, 6627, Campus Universitário, Belo Horizonte, MG CEP 31270-901, Brazil
[c] Instituto Nacional de Ciência e Tecnologia (INCT) de Bioanalítica, Universidade Estadual de Campinas (UNICAMP), Instituto de Química, Departamento de Química Analítica, Cidade Universitária Zeferino Vaz s/n, CEP 13083-970 Campinas, SP, Brazil

ARTICLE INFO

Article history:
Received 4 September 2016
Received in revised form 19 November 2016
Accepted 22 November 2016
Available online 26 November 2016

Keywords:
FIA-TS-FF-AAS
Isotherm
Adsorption
Preconcentration
Poly(vinylpyridine-TRIM)-SiO_2/mercaptopropyltrimethoxysilane

ABSTRACT

A novel hybrid ion imprinted polymer (HIIP) is proposed aiming at the development of an online micro-solid phase preconcentration system of Cd^{2+} coupled to TS-FF-AAS. To evaluate the selective and adsorptive performance of HIIP towards Cd^{2+}, hybrid non-imprinted polymer (HNIP), organic ion imprinted polymer (OIIP), and the inorganic ion imprinted polymer (IIIP) were synthesized and compared with each other. Adsorption capacity of HIIP was 53% higher than HNIP, and dual-site Langmuir–Freundlich isotherm model showed the best fit for data of both polymers. The preconcentration system coupled to TS-FF-AAS was performed by loading 10.0 mL of Cd^{2+} solution at pH 7.5 through 80.0 mg of HIIP packed into a micro-column with posterior online elution using 1.0 mol L^{-1} HCl/ethanol 1:1 (v/v) mixture. The developed method was highly tolerant for other metal ions Zn^{2+}, Pb^{2+}, Cu^{2+}, Co^{2+}, Fe^{2+}, and Hg^{2+} at analyte:interferent (1:50, m/m) ratio and Ca^{2+} and Mg^{2+} at 1:500 (m/m) ratio. Analytical curve ranging from 0.5 to 7.0 μg L^{-1}, limit of detection of 30 ng L^{-1} and preconcentration factor of 14-fold were obtained. Intra-day and inter-day (3 days) experiment precision ($n = 10$) was, respectively, 3.9 and 0.6% (relative standard deviation, RSD), and 4.4 and 2.4% for concentrations of 0.7 and 6.5 μg L^{-1}. Sensitivity of method (Abs L μg^{-1}) was about 3.3, 2.2 and 1.9-fold higher when compared to preconcentration method using HNIP, OIIP and IIIP, respectively, thus clearly showing that hybrid polymer and imprinting process enhance Cd^{2+} adsorption. Addition and recovery experiments ranging from 94 to 106% in mineral, lake water and tap water, urine and cigarette samples attested the feasibility of method for analysis of matrices containing different components. Moreover, the accuracy of method was checked from analysis of certified reference material (DOLT-4, fish liver), being the obtained value of 23.9 ± 0.6 mg kg^{-1} ($n = 3$) statistically equal to the certified value of 24.3 ± 0.8 mg kg^{-1}, by applying Student *t*-test at 95% confidence level.

1. Introduction

Chelating polymers synthesized in the presence of ionic template, i.e., ion imprinted polymers (IIP) were reported for the first time in the mid-1970s by Nishide et al. [1,2]. In this study, chains of poly(4-vinylpyridine) previously synthesized were crosslinked with 1,4-dibromobutane in the presence of metal ions. Although a very high adsorption capacity towards the metal ions has been achieved, the selectivity was somewhat low because the poly(4-vinylpyridine) was not synthesized in the presence of metal ions as templates. Currently, the ionic imprinting process is usually carried out by using an appropriated functional monomer, which forms a complex with ion template and then copolymerized in the presence of crosslinking monomer. Subsequent removal of ion template from polymeric matrix results in recognition sites, which are complementary in size and shape [3,4]. Due to its intrinsic selectivity and adsorptive performance, IIP has been widely used for a large range of applications in analytical science including membrane separations [5], development of electrochemical sensors [6] and flow injection analysis-solid phase extraction (FIA-SPE) systems coupled with spectrochemical analytical techniques including flame atomic absorption spectrometry (FAAS), graphite furnace atomic absorption spectrometry (GF AAS), inductively coupled plasma optical emission spectrometry (ICP OES), inductively coupled plasma mass spectrometry (ICP-MS), and spectroscopy UV–Vis with substantial advantages over commercial non-selective adsorbents such as

* Corresponding author at: Departamento de Química, Universidade Estadual de Londrina (UEL), Rod. Celso Garcia Cid, PR 445 Km 380, Campus Universitário, Londrina, PR CEP 86051-990, Brazil.
E-mail address: ctarleyquim@yahoo.com.br (C.R.T. Tarley).

http://dx.doi.org/10.1016/j.microc.2016.11.013
0026-265X/

Amberlite-XAD, Chelex-100, and octadecyl-C_{18}-silica [7–11]. The use of IIP as adsorbents in SPE has allowed obtaining highly sensitive methods for trace level analysis and in most cases promotes efficient cleanup of sample for removing unwanted interferences. Furthermore, IIP presents some additional advantages, including stability in harsher environments, such as acidic and alkaline medium, organic solvent, temperature and pressure, without decreasing its reusability [12]. Despite recent advances describing the feasibility and reliable use of IIP for separation and preconcentration procedures, the success of analytical method depends upon the type of adopted synthesis. One of the most used approaches for synthesis of IIP is based on bulk polymerization; however, as the main limitations of this method, it can be cited the irregularity of particles in shape and size due to ground process of final material, the poor solubility of ion template (salt) in the imprinting mixture and homogeneity, low removal of ion template from binding sites resulting in bleeding of the materials, selectivity only reasonable due to heterogeneous nature of the binding sites and slow mass transfer [13]. Therefore, efforts have been increasingly made to overcome some of these drawbacks by means of new synthesis approaches of organic polymers, such as precipitation, suspension, emulsion and two-step polymerization [14]. Besides these approaches, the use of grafting process on the surface of inorganic materials [15,16], synthesis of organic ion imprinted polymer using auxiliary chelating [17], hierarchical double-imprinted method using metal ion and cationic surfactant as templates [18], organic ion imprinted polymers (OIIP) using dual functional monomers [19] and hybrid ion imprinted polymers (HIIP) [20] are other examples for obtaining IIP with improved performance in selective SPE procedure of metal ions regarding the bulk method. According to studies reported by Cai and coworkers [19] and Hoai and coworkers [21], a synergic effect and substantial improvement on the selective adsorption of Pb^{2+} and Cu^{2+} were observed using an IIP prepared through suspension polymerization and by using dual functional monomers of methacrylic acid and vinylpyridine in comparison to the use of single functional monomer. Regarding the hybrid ion imprinted polymers, in which the organic and inorganic phases are covalently bonded; one should note that although few studies have been reported so far [20–23], these materials have some outstanding features that can be pointed out, such as high physical and chemical stability, good solvent resistance, low swelling effect and good morphological features [24].

Therefore, inspired in the synergy of dual functional monomers as well as in the features of organic-inorganic hybrid polymers, in the present study, we have prepared for the first time an ion-selective bifunctional hybrid imprinted poly(vinylpyridine-TRIM)-SiO_2/mercaptopropyltrimethoxysilane for its further application in the development of an online micro-solid phase preconcentration of Cd^{2+} coupled to thermospray flame furnace atomic absorption spectrometry (TS-FF-AAS). To the best of our knowledge, the synthesis of proposed ion-selective bifunctional hybrid material as well as its combination with flow injection analysis-solid phase extraction have not been previously reported in the literature. The monomer 4-vinylpyridine (4-VP) and the functional organosilane 3-mercaptopropyltrimethoxylane were chosen bearing in mind their capacity in forming coordination complexes with Cd^{2+} through binding sites of nitrogen from pyridine ring [25] and thiol groups (S—H) from organosilane [26]. The interest in coupling the micro-solid phase preconcentration system with TS-FF-AAS comes from the necessity of monitoring Cd^{2+} ions at very low levels in different samples that promote occupational exposure to human health [27,28]. It should also be pointed out that coupling of flow injection analysis-solid phase extraction with TS-FF-AAS is somewhat limited because the thermospray can only accept very low flow rate, and as a consequence, low sample loading is usually employed, thus leading to reduced improvements in the sensitivity. In this sense, the use of adsorbent with high adsorptive performance, such as the bifunctional hybrid ion imprinted polymer herein developed, is highly efficient to obtain high preconcentration factor even using low sample loading. In order to check the real advantages of HIIP towards the adsorption of Cd^{2+}, hybrid non-imprinted polymer (HNIP), organic ion imprinted polymer (OIIP), and the inorganic ion imprinted polymer (IIIP) were synthesized and compared with each other through a flow injection analysis system coupled to TS-FF-AAS. Upon physical and chemical characterization of four adsorbents, kinetic studies, adsorption isotherms and thermodynamics studies were performed. Finally, figures of merit were obtained and the feasibility of proposed method was evaluated from analysis of real samples (water samples, urine, cigarette and certified reference material).

2. Experimental

2.1. Equipment

The measurements were performed by using an AA-6601 flame atomic absorption spectrophotometer (Shimadzu, Kyoto, Japan) equipped with a cadmium hollow cathode lamp (Hamamatsu Photonics K.K., Hamamatsu City, Japan) and deuterium lamp for background correction. The flame consisted of acetylene and air at 15.0 and 1.8 L min^{-1}, respectively. The cadmium hollow cathode lamp was operated at 8 mA and 228 nm. For construction of the flow injection analysis-solid phase extraction system coupled to TS-FF-AAS, a peristaltic pump (ICP-08 model, Ismatec, Switzerland), a home-made injector commutator made of Teflon® (PTFE, polytetrafluoroethylene), a 0.5 mm i.d. ceramic capillary (Al_2O_3 99.7%) (Friatec, Germany); a 10 cm long and 2.5 cm i.d. (Inconel 600 tube with 72% of Ni, 14–17% of Cr, 6–10% of Fe, 0.15% of C, 1% of Mn and 0.5% of Si, Camacam, Brazil), containing 6 holes of 2.5 mm i.d., and Tygon® tubes were used. The pH of samples was measured by an 826 pH mobile Metrohm (Herisau, Switzerland). The centrifuge (Fanen®, model 206, São Paulo-Brazil) was used for separating phases in the batch experiments. The main functional groups in the materials were identified by Infrared (IR) transmission spectra (KBr pellets), which were recorded on a FTIR-8300 spectrometer (Shimadzu) in the range of 4000–400 cm^{-1}. For the digestion of cigarette and certified reference material (DOLT-4, fish liver), a Milestone Ethos One microwave (São Paulo, Brazil) equipped with 50.0 mL Teflon® vessels was used. The thermal stability of polymeric materials was analyzed on a Perkin Elmer TGA 4000 thermogravimetric instrument ranging in temperature from 30 to 800 °C (scanning rate of 10 °C min^{-1}) at a flow rate of 20.0 mL min^{-1} of nitrogen. The measurements of X-ray diffraction were performed in a PANalytical model X'Pert PRO MPD diffractometer (Almelo, Germany), X-ray diffraction spectra were acquired from a Philips MDR X-ray diffractometer (Eindhoven, Holland) operated with incident X-rays ($\lambda = 1.54060$ Å) with the 2θ angles varying between 5 and 80° with current of 35 mA and voltage of 40 kV. The morphology of polymers was evaluated by using a MIRA field emission scanning electron microscope (FEG-SEM) (Tescan, Mira Model, Czech Republic).

2.2. Chemicals and reagents

All solutions used in this work were prepared in purified water using a Milli-Q purification system (Millipore, Bedford, MA, USA) (resistivity higher than 18.2 MΩ cm). In order to avoid any metal contamination in blank solutions, all laboratory glassware was kept overnight in a 10% (v/v) HNO_3 solution. Stock solution of 1000 mg L^{-1} Cd^{2+} (NIST) was used for the preparation of working solution of 1.0 mg L^{-1} Cd^{2+} by making appropriate dilutions with purified water. Reagents used for polymer syntheses were: 4-vinylpyridine (4-VP) (95%) as functional monomer, 3-mercaptopropyltrimethoxysilane (3-MPTMS) (95%) as functional organosilane, 3-(trimethoxysilyl)propyl methacrylate (KH570) (>98%) as coupling reagent for organic and inorganic phases, trimethylolpropane trimethacrylate (TRIM) as crosslinking reagent, 2,2′ azo-bis-isobutyronitrile (AIBN) as radical initiator and tetraethoxysilane (TEOS) (98%) as functional precursor and were

acquired from Sigma-Aldrich (Steinheim, Germany) and used without further purification. $Cd(NO_3)_2 \cdot 4H_2O$ used as ion template was acquired from Vetec (Rio de Janeiro, Brazil). The solutions of Ca^{2+}, Mg^{2+}, Zn^{2+}, Pb^{2+}, Cu^{2+}, Co^{2+} and Fe^{2+} used in interference studies were obtained from their respective nitrate salts, while the solution of Hg^{2+} was prepared from chloride salt.

2.3. Synthesis of hybrid ion imprinted polymer (HIIP), hybrid non-imprinted polymer (HNIP), organic ion imprinted polymer (OIIP) and inorganic ion imprinted polymer (IIIP)

To synthesize the HIIP, 2.40 mmol (0.7398 g) of $Cd(NO_3)_2 \cdot 4H_2O$ was dissolved in 40.0 mL of ethanol into a round-bottom flask, followed by addition of 0.04 mol (4.30 mL) of 4-vinylpyridine and 0.02 mol (4.00 mL) of 3-mercaptopropyltrimethoxysilane. Afterwards, 300 mg of 2,2′ azo-bis-isobutyronitrile, 0.02 mol (4.75 mL) of 3-(trimethoxysilyl)propyl methacrylate as coupling reagent and 0.015 mol (5.0 mL) of trimethylolpropane trimethacrylate were added to the mixture. The mixture was then purged with nitrogen gas for 10 min and heated at 60 °C for 30 min in an oil bath. In the next step, 8.0 mL of tetraethoxysilane previously dissolved in ethanol and 3.8 mL of 1.0 mol L^{-1} NaOH were added to the flask. The mixture was again heated at 60 °C for 24 h to allow the polymerization. The obtained hybrid polymer was dried at 60 °C, ground and sieved to obtain particles with diameters ranging from 106 to 150 μm. The representative scheme of HIIP preparation is shown in Fig. 1. In order to remove Cd^{2+} ions from polymeric matrix, successive washings with 2.0 mol L^{-1} HCl were performed until no more Cd^{2+} was detected by TS-FF-AAS. The blank

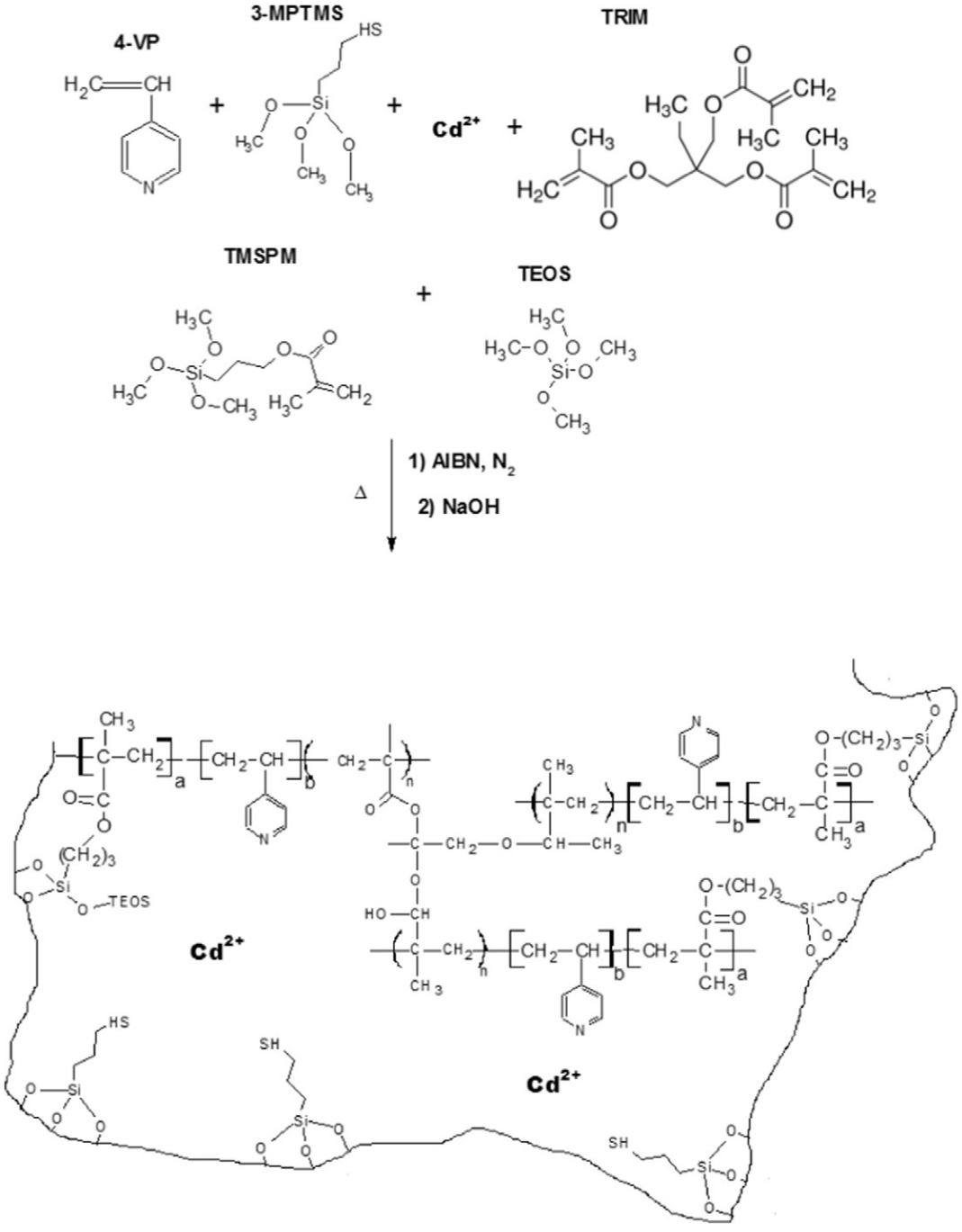

Fig. 1. Representative scheme of the HIIP preparation.

polymer, i.e., the hybrid non-imprinted polymer (HNIP) was synthesized in similar way to HIIP, except by absence of $Cd(NO_3)_2 \cdot 4H_2O$.

Synthesis of organic ion imprinted polymer (OIIP) was performed by dissolving 2.40 mmol (0.7398 g) of $Cd(NO_3)_2 \cdot 4H_2O$ in 50.0 mL of ethanol followed by addition of 0.04 mol (4.30 mL) of 4-vinylpyridine. Afterwards, 300 mg of 2,2′ azo-bis-isobutyronitrile and 0.015 mol (5.00 mL) of trimethylolpropane trimethacrylate were added to mixture, which was then purged with nitrogen gas for 10 min and heated at 60 °C for 24 h in an oil bath. Finally, the polymer was dried, ground, sieved and washed similarly to procedure adopted for HIIP.

For the synthesis of inorganic ion imprinted polymer (IIIP), the sol-gel processing was used. An amount of 2.40 mmol (0.7398 g) of $Cd(NO_3)_2 \cdot 4H_2O$ dissolved in 40.0 mL of ethanol was mixed with 0.02 mol (4.00 mL) of 3-mercaptopropyltrimethoxysilane. Then, 0.02 mol (4.75 mL) of 3-(trimethoxysilyl)propyl methacrylate, 0.04 mol (8.00 mL) of tetraethoxysilane dissolved in ethanol and 3.8 mL of 1.0 mol L^{-1} NaOH as catalyst were added to the mixture. The polymerization occurred at 60 °C for 24 h in oil bath. In a similar way to OIIP and HIIP, the IIP was also dried, ground, sieved and washed with 2.0 mol L^{-1} HCl for Cd^{2+} removal.

2.4. Adsorption kinetics

The effect of time on the adsorption of Cd^{2+} on HIIP and HNIP was carried out in a batch experiment, which allowed to insight into the adsorption mechanism and the rate-controlling steps. Briefly, 20.0 mL of 5.0 mg L^{-1} Cd^{2+} was prepared at pH 7.56 buffered with 0.048 mol L^{-1} Tris-HCl buffer solution and stirred at 130 rpm with 100 mg of polymers at different time intervals (1, 3, 5, 10, 15, 20, 30, 40, 50 and 60 min). After the contact time elapsed, the mixture was centrifuged for 10 min at 2000 rpm, and the supernatants were analyzed for Cd^{2+} concentration using FAAS. All the experiments were performed in triplicate. The content of Cd^{2+} adsorbed onto polymers (mg g^{-1}) at different intervals was determined according to Eq. (1).

$$Q_t(mg/g) = \frac{(C_i - C_f).V}{m} \quad (1)$$

where Q_t is the amount of Cd^{2+} (mg g^{-1}) adsorbed on the polymers at determined time (min); C_i and C_f are the initial and final concentrations of Cd^{2+}, respectively (mg L^{-1}), determined by FAAS; V is the volume of solution (mL); and m is the mass of the polymer (g). In order to investigate rate determining step, data from the effect of contact time were fitted to common linear adsorption kinetic models, pseudo-first-order, pseudo-second order, Elovich and intraparticle diffusion [29,30].

2.5. Adsorption isotherms

The effect of initial Cd^{2+} concentration on its adsorption by polymers was evaluated under equilibrium condition from batch adsorption isotherms. From these studies, the adsorption capacities of polymers as well as a better insight into the adsorption mechanism involving different binding sites were obtained.

For the HIIP, 100.0 mg of polymer was stirred with 20.0 mL of Cd^{2+} solutions at pH 7.56 buffered with 0.048 mol L^{-1} Tris-HCl buffer solution for 30 min with increasing concentration varying from 2.0 to 28.0 mg L^{-1}. Isotherm for HNIP was built by varying the Cd^{2+} concentration from 2.5 to 16.0 mg L^{-1}. These concentrations are different than the ones employed for HIIP due to lower capacity of the HNIP towards Cd^{2+}. Then, the mixture was centrifuged for 10 min and the supernatant was analyzed by FAAS. The adsorption capacity (mg g^{-1}) was calculated according to Eq. (2).

$$Q_e(mg/g) = \frac{(C_i - C_e).V}{m} \quad (2)$$

where Q_e is the amount of Cd^{2+} (mg g^{-1}) adsorbed on the polymers at equilibrium time (min) and C_i and C_e are the respective initial and equilibrated concentrations of Cd^{2+} (mg L^{-1}), V is the volume of solution (mL); and m is the mass of polymer (g). In a similar way to kinetic data, all the experiments were performed in triplicate. Experimental isotherm data were fitted with non-linear Langmuir, non-linear Freundlich, and single-site and dual-site Langmuir-Freundlich adsorption models [31,32].

2.6. Evaluation of template effects on HIIP in the presence of interfering cations

In order to evaluate the imprinting effect of Cd^{2+} on bifunctional hybrid imprinted polymer, competitive adsorption of binary solutions Cd^{2+}/Pb^{2+}, Cd^{2+}/Zn^{2+} and Cd^{2+}/Cu^{2+} was carried out in batch experiments using HIIP and HNIP. That is, 100 mg of polymers was dispersed in 20.0 mL of binary solutions at 5.0 mg L^{-1} concentration under pH 7.56 buffered with 0.048 mol L^{-1} Tris-HCl buffer, being continuously stirred for 30 min and then centrifuged for 10 min at 2000 rpm. Concentration of supernatant was further measured by FAAS. Distribution (K_d), selectivity (k_{HIIP}, k_{HNIP}) and relative selectivity (k′) coefficients of Cd^{2+} with respect to Pb^{2+}, Zn^{2+} and Cu^{2+} were determined according to Eqs. (3)–(6), respectively [33].

$$K_d = \frac{(C_i - C_f)}{C_f} \times \frac{V}{M}, \quad (3)$$

Where C_i and C_f represent the initial and final solution concentrations, V is the solution volume (mL), and M is the polymer mass (mg);

$$k_{HIIP} = \frac{K_d Cd^{2+}}{K_d\left(Pb^{2+}, Zn^{2+} or - Cu^{2+}\right)} \quad (4)$$

$$k_{HNIP} = \frac{K_d Cd^{2+}}{K_d\left(Pb^{2+}, Zn^{2+} or - Cu^{2+}\right)} \quad (5)$$

$$k\prime = \frac{k_{HIIP}}{k_{HNIP}} \quad (6)$$

2.7. Thermodynamic parameters of Cd^{2+} adsorption on HIIP and HNIP

Thermodynamic parameters (ΔH), entropy (ΔS) and Gibbs free energy (ΔG) were determined, so the nature of interaction of Cd^{2+} on HIIP and HNIP could be evaluated. The experiments were carried out under stirring for 30 min at six different temperatures (303.15, 313.15, 323.15, 333.15, 343.15 and 353.15 K) and 20.0 mL of 5.0 mg L^{-1} Cd^{2+} solution with 100 mg of polymers under pH 7.56 buffered with 0.048 mol L^{-1} Tris-HCl buffer. Concentration of supernatant was further measured by FAAS. From the graph of lnKd versus 1/T (van't Hoff plot), described by Eq. (7), the parameters ΔH and ΔS were obtained from the intercept and slope of the graph, respectively.

$$\ln K_d = -\frac{\Delta H}{R}\left(\frac{1}{T}\right) + \frac{\Delta S}{R} \quad (7)$$

where, the distribution coefficient (Kd) (L g^{-1}) at six different temperatures corresponds to the ratio (Qe, mg g^{-1})/(supernatant concentration, Ce, mg L^{-1}), R is the universal gas constant (R = 8.314 J mol^{-1} K^{-1}) and T is the temperature in Kelvin. The Gibbs free energy was determined for the adsorption process of Cd^{2+} at

303.15 K using Eq. (8) [34].

$$\Delta G = \Delta H - T\Delta S \quad (8)$$

2.8. Online preconcentration procedure of Cd^{2+} coupled to TS-FF-AAS

The online preconcentration system coupled to TS-FF-AAS operated in a time-based mode [26] was carried out by percolating 10.0 mL of sample (buffered with 0.048 mol L^{-1} Tris-HCl buffer, pH 7.56) at a flow rate of 5.0 mL min^{-1} through 80.0 mg of HIIP packed into a polyethylene micro-column (5 cm × 0.5 cm, containing cotton in each edge to prevent loss of the material). After the preconcentration step, elution was performed by switching the injector to the elution position using 1.0 mol L^{-1} HCl/ethanol 1:1 (v/v) mixture at 0.5 mL min^{-1} flow rate, where the desorbed Cd^{2+} ions were transported on-line towards TS-FF-AAS. The use of ethanol in the eluent acid is recommended to improve the spray formation. The analytical response was taken as absorbance (peak height).

2.9. Sample preparation

A known amount of cigarette and certified reference material (DOLT-4, fish liver) was weighted and transferred to Teflon® flasks. Then, 10.0 mL of concentrated HNO_3 and 4.0 mL of 30% H_2O_2 were added and the mixture was kept at rest overnight. The mineralization of samples was performed by using microwave radiation at 700 W and adopting the following steps: heating up to 80 °C, maintenance time of 5 min at 80 °C - heating ramp of 10 min up to 120 °C, maintenance time of 5 min at 120 °C – heating ramp of 10 min up to 200 °C, maintenance time of 20 min at 200 °C. After mineralization, solutions were transferred to glass flask and heated on a hot plate until almost dry. Then the residue was dissolved in 0.048 mol L^{-1} Tris-HCl buffer solution at pH 7.56. For urine, which voluntary healthy people kindly provided, 25.0 mL of sample was mineralized exactly equal to solid samples.

Lake water sample was collected in polypropylene bottles from Igapó Lake located in Londrina city, Brazil, filtered under vacuum using 0.45 μm cellulose acetate membranes with pH adjusted to 7.56 with 0.048 mol L^{-1} Tris-HCl buffer solution. Tap and mineral waters were collected from State University of Londrina campus and local supermarkets, respectively, and their pH was also adjusted to 7.56. For all samples, the analyses were carried out in triplicate.

3. Results and discussion

3.1. FT-IR

The functional groups present in the polymers (HIIP, HNIP, IIIP e OIIP) were confirmed from FT-IR spectra (Fig. 2). As seen, for all polymers a typical band at 3440 cm^{-1} was noticed, which is attributed to O—H stretch from adsorbed water or by the presence of silanol groups. The band at 2936 cm^{-1} is assigned to C-axial deformation of C—H from polymeric chain [35]. The band at 1640 cm^{-1} was observed for the four polymers, which is assigned to deformation (O—H—O) from adsorbed water or by vinyl groups still present in the polymers containing the organic portion [36,37]. For the IIIP, the presence of thiol group (S—H) was attributed to low intense band at 2557 cm^{-1}, while the band at 1412 cm^{-1} is attributed to symmetric angular deformation of Si-CH_2 present in both coupling agent 3-(trimethoxysilyl)propyl methacrylate and 3-MPTMS [38].

For the organic polymer OIIP, two low intensity bands at 1259 and 1166 cm^{-1} ascribed to C—O stretching from trimethylolpropane trimethacrylate (TRIM) as crosslinking were observed. Clearly, the overlapping of these peaks in the hybrid polymers of inorganic polymer by

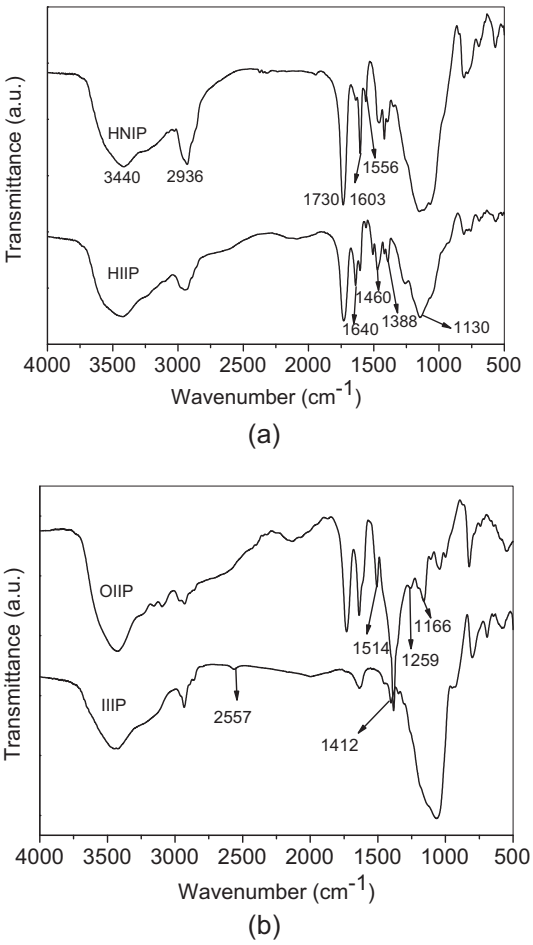

Fig. 2. Infrared spectrum for (a) HIIP and HNIP and (b) OIIP and IIIP.

broadband varying from 950 to 1280 cm^{-1} can be observed, which is attributed to asymmetric stretching of Si—O—Si and Si—O—H [22,35,36]. As expected, the intense band at 1730 cm^{-1} is most likely assigned to C ═O stretching from trimethylolpropane trimethacrylate (TRIM). The confirmation of organic monomer 4-vinylpyridine (4-VP) in the polymeric matrix of OIIP was attested by the band at 1388 cm^{-1}, only found in HIIP, HNIP and OIIP materials, ascribed to C—N stretching from the pyridine ring [39].

In addition, this band was considerably much larger for OIIP due to the higher presence of 4-vinylpyridine (4-VP). A band of middle intensity at approximately 1460 cm^{-1} and another of low intensity at 1420 cm^{-1} have been observed for HIIP and HNIP, which are ascribed to C ═C stretching from ring of 4-vinylpyridine and two bands at 1556 and 1603 cm^{-1} attributed to C ═N stretching from ring.

3.2. Thermal analysis and X-ray diffraction

Thermal stability of polymers was determined by means of TGA and DTG (Fig. 3a,b). As can be observed from TGA, the ceramic yield achieved for the hybrid polymers HIIP and HNIP was intermediary compared to the OIIP and IIIP ones. The weight losses for the HIIP, HNIP, OIIP and IIIP until 800 °C were found to be 27.2, 36.0, 72.9 and 11.3%, respectively. In the temperature range varying from 30 to 130 °C, weight loss ranging from 4.3 to 7.9% is attributed to physically adsorbed water. From DTG, for the OIIP, a weight loss in the temperature range of 300–450 °C was observed, which is attributed to decomposition of polymeric chain of 4-vinylpyridine and TRIM [40]. Regarding IIIP, the DTG shows an event at 547 °C with low weight loss (~5%) ascribed to dehydration of residual silanol groups, decomposition of 3-MPTMS at 227 °C,

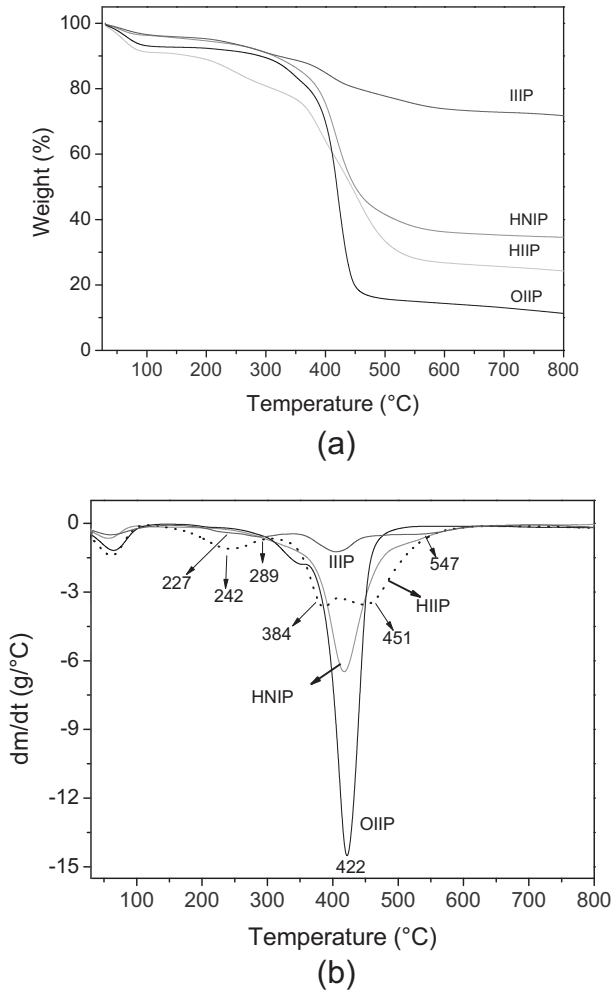

Fig. 3. Thermogravimetric (a) and derivative curves (b) for HIIP, HNIP, OIIP and IIIP.

decomposition of ester linkage from 3-(trimethoxysilyl)propyl methacrylate at 289 °C and degradation of Si—C bonds and redistribution of Si—O at 407 °C [36,37,41]. When thermal analysis of HIIP was evaluated, two degradation regions in the range of 350–500 °C as compared to OIIP and IIIP were observed. Thus, it seems that the well-defined degradation of polymeric chain of 4-vinylpyridine and TRIM took place at 384 °C, while the degradation of inorganic matrix (Si—C bonds) and redistribution of Si—O took place at 451 °C. Moreover, the decomposition of 3-MPTMS for the HIIP took place at higher temperature (242 °C) as compared to IIIP (227 °C).

The thermal behavior of HNIP was somewhat similar to OIIP, except by higher ceramic yield due to the presence of inorganic matrix. Therefore, different from thermal behavior of HIIP, the non-imprinted polymer shows only an event at 350–500 °C, which indicates that inorganic and organic portions are densely connected making the whole chain stiffer. One should still note that HNIP presents higher thermal stability and ceramic yield than HIIP most likely due to more strengthening of the chemical bonds in the backbone chain of organic and inorganic portion as a result of absence of template ion [18,22].

The X-ray diffractograms of polymers are depicted in Fig. 4. The XRD patterns of polymers exhibited a broad peak in the range of 15–30°, which can be attributed to inorganic amorphous fraction of polymers represented by siloxane domains as well as by semi-crystalline organic fraction [22,42]. It is worth pointing out that apart from the amorphous fraction of siloxane domains noticed in the hybrid and inorganic materials, the organic one presented a halo at 43° attributed to amorphous phase of organic matrix. Such peak is not present in the IIIP material,

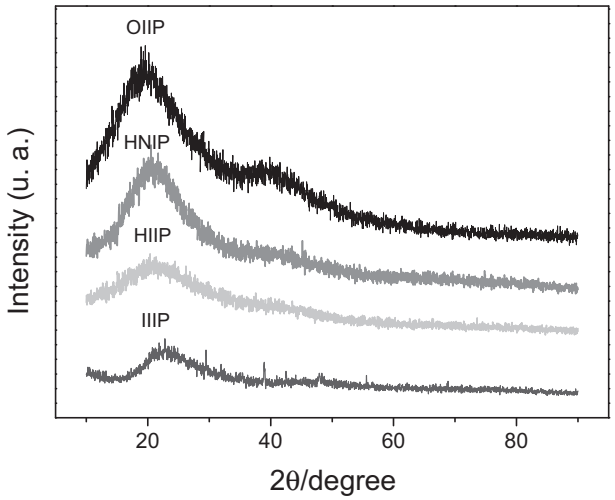

Fig. 4. X-ray diffraction of HIIP, HNIP, OIIP and IIIP.

but it is present in the hybrid materials with intermediary intensity regarding the OIIP material, which in turn also confirms the formation of hybrid material.

3.3. Morphological features of materials

Fig. 5 shows SEM images of materials. As one can see, the morphological profile of materials is different from each other mainly if the OIIP and IIIP ones are considered (Fig. 5c,d). For OIIP material, a rough surface with more cohesive particles and high aggregation was observed, in contrast to IIIP particles, which presented irregular shapes and a flat surface, very similar to those materials based on silica matrix [43]. The hybrid polymers (HIIP and HNIP) showed, as expected, an intermediary roughness regarding the OIIP and IIIP. However, one should note from a more detailed interpretation that HIIP surface is somewhat rougher than HNIP, playing an important role in the adsorption process. Such result can be rationalized bearing in mind that the presence of template ion during HIIP synthesis may lead to a higher solubility of Cd^{2+} and functional monomers (metallic complex) into the growing polymeric chain and lower solubility in the porogenic solvent and, as a consequence, making the removal of solvent from interstices easier, thus giving rise to a rougher surface [14].

3.4. Adsorption kinetics

A set of adsorption experiments as mentioned in Section 2.4 was carried out as function of time to evaluate the adsorption kinetics. It was observed (data not shown) that equilibrium for the adsorption of Cd^{2+} on HIIP and HNIP was achieved at 20 and 30 min, respectively. The fast adsorption kinetics may be a strong indicative that the materials, especially the HIIP, are very suitable for the development of an on-line preconcentration system from a large volume of solutions. The adsorption kinetic constant and the regression coefficients for the non-linear fit of pseudo-first-order, pseudo-second-order, Elovich and intraparticle diffusion model are summarized in Table 1. As can be observed, the adsorption kinetics of Cd^{2+} on HIIP and HNIP follows the pseudo-second-order model ($R^2 = 0.999$). Moreover, the experimental adsorption capacities, $Q_{experimental}$, for HIIP (0.530 mg g^{-1}) and HNIP (0.856 mg g^{-1}) were far closer to those values predicted by the model, 0.552 mg g^{-1} for HIIP and 0.900 mg g^{-1} for HNIP. This model recognizes that adsorption takes place in binding sites with different energies, as well as the rate of occupation of adsorption sites is proportional to the square of the number of unoccupied sites [44]. The different binding sites may be ascribed to sulfur atom from functional organosilane 3-MPTMS, and nitrogen atom from 4-vinylpyridine, in

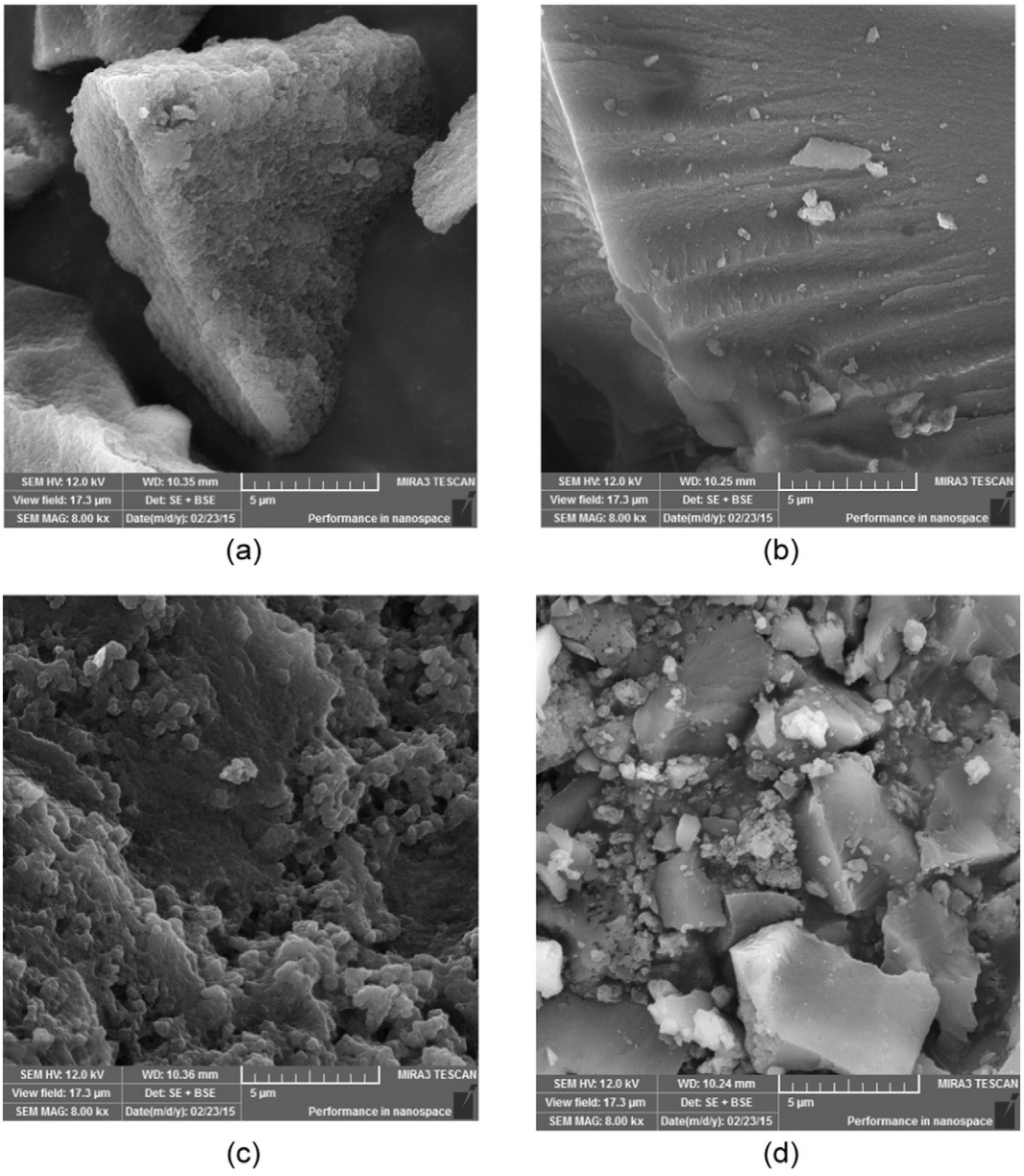

Fig. 5. SEM images of (a) HIIP, (b) HNIP, (c) OIIP and (d) IIIP. Magnification of 8.000 times.

Table 1
Kinetic parameters for the adsorption of Cd(II) on HIIP and HNIP. $Q_{exp} = 0.5030$ mg g^{-1} for HIIP, 0.856 mg g^{-1} for HNIP.

	Pseudo-first-order $\log(Q_e - Q_t) = \log Q_e - \frac{k_1}{2.303} t$			Pseudo second-order $\frac{t}{Q_t} = \frac{1}{k_2 Q_e^2} + \frac{1}{Q_e} t$		
Hybrid polymers	k_1	Q_e	R^2	k_2	Q_e	R^2
HIIP	0.122	0.221	0.914	1.262	0.552	0.999
HNIP	0.107	0.302	0.934	0.758	0.900	0.999
	Elovich $Q_t = \frac{1}{\beta} \ln(\alpha\beta) + \frac{1}{\beta} \ln t$			Intraparticle diffusion $Q_t = k_{id}\, t^{1/2} + C$		
Hybrid polymers	β	α	R^2	k_{id}	C	R^2
HIIP	14.925	5.233	0.992	0.120	0.146	0.993
				0.047	0.322	0.947
HNIP	10.548	27.446	0.981	0.103	0.447	0.956
				0.032	0.680	0.773

k_1: It is constant for pseudo-first-order of adsorption process (min^{-1}); Qe: It is the adsorption capacity in the equilibrium (mg g^{-1}); k_2: It is constant for pseudo-second-order of adsorption process (g mg^{-1} min^{-1}); β: It is associated with the surface coverage extension and the activation energy of chemisorption (g mg^{-1}); α: is the initial adsorption rate constant (min^{-1}· mg g^{-1}); K_{id}: is the coefficient of diffusion internal (mg g^{-1} $min^{-1/2}$); C_i: is a constant related to the thickness of the boundary layer (mg g^{-1}).

which are capable to interact with Cd^{2+}. It is worth noting that the Elovich model also presented good fit to the experimental data, thus confirming the pseudo-second-order model, whereas the adsorption of Cd^{2+} occurs, in fact, on the energetically heterogeneous surface of hybrid polymers [45]. The good fit of intraparticle diffusion model to the experimental kinetic data allows us to predict the nature of transport of Cd^{2+} ions towards surface of materials. As shown in Table 1, two linear plots were defined, whose parameter C (constant related to the thickness of the boundary layer) is far from zero, suggesting that adsorption process is controlled by the quick external surface adsorption limited by boundary layer in a shorter time (first linear plot) and intraparticle diffusion into pores of material (second linear plot) [30].

3.5. Adsorption isotherms

Fig. 6 depicted the adsorption isotherms of Cd^{2+} on HIIP and HNIP under equilibrium condition. The maximum experimental adsorption capacity (MEAC) for HIIP and HNIP was calculated to be 2.67 and 1.72 mg g^{-1}, respectively. The higher MEAC for HIIP can be used as a primary parameter to evaluate the efficiency of imprinting effect created in the polymer; however, one should note that the selectivity of HIIP towards the adsorption of Cd^{2+} in comparison with HNIP must be confirmed from competitive studies as will be further demonstrated in Section 3.6. The fit of theoretical models to experimental adsorption isotherm, allows, in a similar way to the kinetic models, to understand the nature of adsorption. Table 2 shows the adsorption constant, regression coefficients and the maximum adsorption capacity (mg g^{-1}) for non-linear Langmuir, non-linear Freundlich, single-site and dual-site Langmuir-Freundlich adsorption models. Taking into account the higher regression coefficients, 0.997 and 0.999 for HNIP and HIIP, respectively, as well as the similarity of MEAC to those theoretical values ($b_1 + b_2$), 1.75 and 2.69 mg g^{-1}, the adsorption isotherm can be described by the dual-site Langmuir-Freundlich adsorption model. Such model is very useful to identify the presence of two-adsorption sites with different affinities towards adsorbate, while the single-site Langmuir-Freundlich adsorption model allows to evaluate the presence of heterogeneous and homogeneous binding sites, but it fails in describing the existence of two-adsorption sites with different affinities [32]. Therefore, for HIIP the adsorption of Cd^{2+} ascribed to $b_1 = 0.505$ mg g^{-1} and $b_2 = 2.187$ mg g^{-1} takes place in binding sites with very different affinities assigned to K_1 and K_2 of 12.39 and 0.257 L g^{-1}, respectively. This finding shows that for low initial concentration of Cd^{2+} the adsorption occurs mostly in higher-affinity sites ($b_1 = 0.505$ mg g^{-1} and $K_1 = 12.39$ L g^{-1}) on the HIIP, probably in the S—H or S atoms present in the imprinted cavity. For higher concentration of Cd^{2+}, the adsorption takes place in lower-affinity sites ($b_2 = 2.187$ mg g^{-1} and $K_2 = 0.257$ L g^{-1}), very likely on the nitrogen atom from the 4-vinylpyridine, in which presents lower affinity to Cd^{2+} regarding sulfur atom [46].

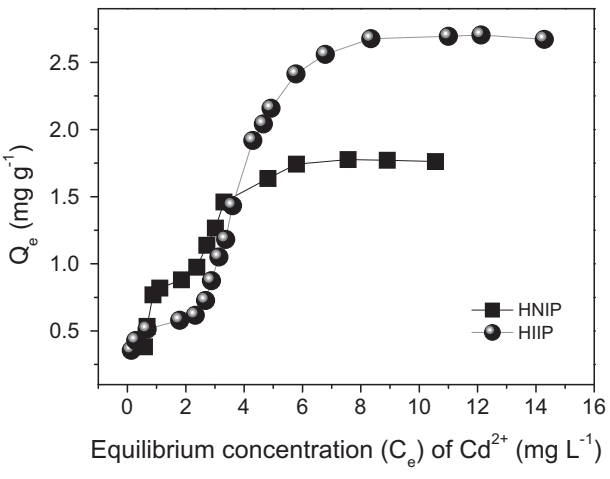

Fig. 6. Adsorption isotherms of Cd^{2+} on HIIP and HNIP.

The achieved results for HNIP, on the other hand, demonstrates that adsorbed amounts of Cd^{2+} on two sites are very similar (0.915 and 0.839 mg g^{-1}), but for low initial concentration of Cd^{2+} the adsorption occurs in lower-affinity sites (0.328 L g^{-1}), mostly in nitrogen atom. In the light of these results, we can infer the absence of imprinted cavity for HNIP with higher-affinity sites; even in the condition at which the free sites are significantly greater than the Cd^{2+} in solution.

3.6. Selectivity of HIIP through competitive adsorption in the presence of interfering cations

Table 3 shows the distribution coefficient (K_d), selectivity coefficient (k) and the relative selectivity coefficient (k´) with respect to Cd^{2+} and other metal ions using HIIP and HNIP. Pb^{2+}, Zn^{2+} and Cu^{2+} were chosen as competitive metallic ions because they are divalent ions likewise to Cd^{2+} and capable to interact with binding site of polymer ascribed by the thiol group and nitrogen from the pyridine ring. It can be clearly observed from comparison of selectivity coefficient (k) of HIIP and HNIP for the binary system Cd^{2+}/Pb^{2+}, Cd^{2+}/Zn^{2+}, Cd^{2+}/Cu^{2+} that the selectivity of HIIP towards the adsorption of Cd^{2+} in the presence of interfering cations is much higher than the HNIP, thus reflecting in relative selectivity coefficients (k´) higher than one unit. From these results, the imprinting effect created during polymer synthesis may improve the selectivity of polymer by 2.17 to 3.6-fold to Cd^{2+} over Pb^{2+}, Zn^{2+} and Cu^{2+} ions. One should note that the K_d value for Zn^{2+} is too much high, which mostly likely is attributed to strong interaction with nitrogen from pyridine ring. Anyway, the K_d values were too much higher for the HNIP, which clearly reflects the imprinting effect created in the HIIP.

3.7. Thermodynamic parameters of Cd^{2+} adsorption on HIIP and HNIP

By plotting the van't Hoff equation under different temperatures (303.15, 313.15, 323.15, 333.15, 343.15 and 353.15 K), a linear relationship was observed, with linear correlation coefficients of 0.995 and 0.991 for HIIP and HNIP, respectively. The obtained values for ΔH (kJ mol^{-1}) and ΔS (k^{-1} J mol^{-1}) were found to be 6.1 and 28.9 for HIIP and 15.8 and 65.4 for HNIP. The positive values of ΔH confirm the endothermic nature of the adsorption process, while the positive ΔS values indicate an increase in the system disorder at the solid/liquid interface during the Cd^{2+} adsorption. The Gibbs free energy (ΔG) was determined at 303.15 K, yielding the negative values of −2.63 and −3.88 (kJ mol^{-1}) for HIIP and HNIP, respectively, demonstrating the energetically favorable Cd^{2+} adsorption process. The increase of Cd^{2+} adsorption with increasing temperature can be attributed to the dehydration process of Cd^{2+} that takes place before the adsorption of Cd^{2+}, which usually requires energy [47,48]. This same phenomenon may be used to explain the positive ΔS values, once the dehydration of water molecules bonded to Cd^{2+} implies in structural changes between adsorbate and adsorbent, and as consequence, the increase in the disorder at solid/liquid interface.

From the obtained ΔH values, we can infer the nature of adsorption process. It is well-known that values of energy are associated with the type of interaction between adsorbate and adsorbent. Electrostatic interactions through chemical ion-exchange involve low adsorption energy (8–16 kJ mol^{-1}) and van der Walls interactions, i.e. interaction of physical nature, such as induced ion-dipole and dipole-dipole, the energy is very low, usually below 8 kJ mol^{-1} [49,50]. The achieved results are somewhat expected, because the interactions of Cd^{2+} with HNIP can be explained by means of ion-exchange, which is not characterized as a selective process. On the other hand, for HIIP, van der Waals interactions play an important role in the retention of Cd^{2+}, once at pH 7.56 cadmium exists in $Cd(OH)^+$ and $Cd(H_2O)_6^{2+}$ forms, and thus, it is expected that these species interact with binding sites of polymer through

Table 2
Non-linear Langmuir, non-linear Freundlich, single-site and dual-site Langmuir-Freundlich constants for the adsorption of Cd(II) on HIIP and HNIP. Q_{exp} = 2.67 mg g^{-1} for HIIP, 1.72 mg g^{-1} for HNIP.

Models	Hybrid polymers HIIP	HNIP
Non-linear Langmuir		
$Q_{eq} = KbC_{eq}/(1 + KC_{eq})$		
K	0.121	0.432
b	4.805	2.171
R^2	0.878	0.955
RMSE	1.778	0.142
Non-linear Freundlich		
$Q_{eq} = KC_{eq}{}^{1/n}$		
K	0.681	0.759
n	1.726	2.445
R^2	0.845	0.912
RMSE	2.297	0.274
Single-site Langmuir-Freundlich		
$Q_{eq} = b(KC_{eq})^{n_1}/1 + (KC_{eq})^{n}$		
K	0.285	0.423
b	2.783	2.276
n	3.355	0.996
R^2	0.951	0.955
RMSE	0.723	0.142
Dual-site Langmuir-Freundlich		
$Q_{eq} = \frac{b_1(K_1C_{eq})^{n_1}}{1+(K_1C_{eq})^{n_1}} + \frac{b_2(K_2C_{eq})^{n_2}}{1+(K_2C_{eq})^{n_2}}$		
K_1	12.390	0.328
K_2	0.257	1.650
b_1	0.505	0.915
b_2	2.187	0.839
n_1	1.601	6.383
n_2	5.165	5.988
R^2	0.999	0.9983
RMSE	0.016	0.120

In the Langmuir, Freundlich and Langmuir-Freundlich equations: K (Langmuir), $K_{1,2}$ (Langmuir-Freundlich) (L g^{-1}), K (Freundlich) (mg g^{-1}) (L g^{-1}) - adsorbate – adsorbent affinities, b, $b_{1,2}$ - maximum adsorption capacities (mg g^{-1}), and n, $n_{1,2}$ - intensities or degrees of favorability for adsorption. RMSE: It is the root-mean-square deviation.

weak intermolecular forces as recognized by the tailor-made process on ionic imprinted polymer.

3.8. Optimization of on-line micro-solid phase preconcentration of Cd^{2+} coupled to TS-FF-AAS using factorial design, response surface methodology and Doehlert matrix

The use of two-level factorial design as exploratory designs combined with Doehlert matrix and response surface methodology has been used as a very efficient tool for optimization, which results in fewer experiments required [51]. The studied factors that play an important role in the preconcentration system, as well as their levels and the analytical responses (absorbance as peak height) obtained from a full 2^4 factorial design are summarized in Table 4. For the 2^4 factorial design, the concentration of Cd^{2+}, preconcentration volume and flow rate were set to 5.0 μg L^{-1}, 10.0 mL and 5.0 mL min^{-1}, respectively. It is worth emphasizing that because thermospray only accept very low flow rate, the flow rate was set at 5.0 mL min^{-1}, as a compromise between elution flow rate, sample throughput, detectability and sample consumption.

The significance of factors on the preconcentration system was graphically evaluated from the Pareto chart (Fig. 7) performed at a confidence level of 95%. From this chart, it can be observed that all

Table 3
Selectivity parameters for the competitive adsorption on the HIIP and HNIP.

Hybrid polymers	K_d		K	k'
	Cd^{2+}	Pb^{2+}		
HIIP	360.057	32.550	11.062	
HNIP	643.336	211.668	3.039	3.64
	Cd^{2+}	Zn^{2+}		
HIIP	421.981	460.775	0.927	
HNIP	547.741	1282.766	0.427	2.17
	Cd^{2+}	Cu^{2+}		
HIIP	429.054	67.229	6.382	
HNIP	724.654	360.763	2.009	3.18

K_d – distribution coefficient; K – selectivity coefficient; k' – relative selectivity coefficient.

Table 4
Factors, their levels and responses obtained in the 2^4 factorial design.

Factors			Levels Low (−)		High (+)	
pH			4.0[a]		8.0[b]	
Buffer solution concentration (BSC) (mol L^{-1})			0.001		0.1	
Eluent concentration (EC) (mol L^{-1})[c]			0.3		1.0	
Adsorbent mass (AM) (mg)			40		80	
Experiments	pH	BSC	ED	AM	Absorbance (peak height)	
1	−1	−1	−1	−1	0.091	0.093
2	1	−1	−1	−1	0.168	0.172
3	−1	1	−1	−1	0.089	0.085
4	1	1	−1	−1	0.180	0.177
5	−1	−1	1	−1	0.091	0.095
6	1	−1	1	−1	0.126	0.126
7	−1	1	1	−1	0.073	0.070
8	1	1	1	−1	0.233	0.227
9	−1	−1	−1	1	0.084	0.084
10	1	−1	−1	1	0.200	0.209
11	−1	1	−1	1	0.051	0.050
12	1	1	−1	1	0.143	0.139
13	−1	−1	1	1	0.085	0.086
14	1	−1	1	1	0.492	0.496
15	−1	1	1	1	0.111	0.103
16	1	1	1	1	0.400	0.410

[a] Acetate/acetic acid buffer.
[b] Tris-HCl buffer.
[c] Eluent HCl in ethanol (1:1, v/v).

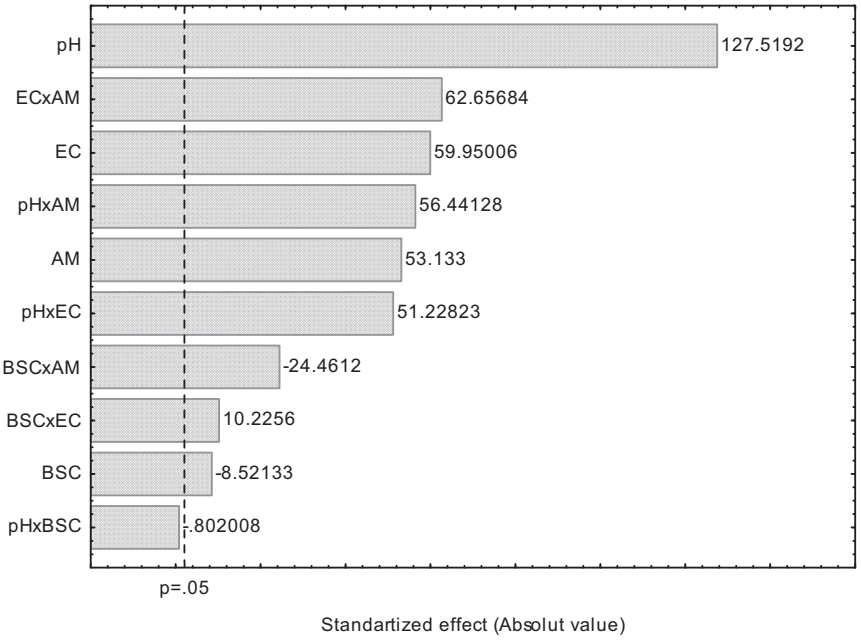

Fig. 7. Pareto chart obtained from the 2^4 factorial design.

experimental factors were significant. The sample pH was the most significant factor with standardized effect of 127.51, thus indicating the analytical signal improved when pH was modified towards greater values (4.0 to 8.0). At higher pH the binding sites of hybrid polymer i.e., the thiol group and nitrogen from the pyridine ring are at their deprotonated form, thus making easier the interaction with $Cd(OH)^+$ and $Cd(H_2O)_6^{2+}$. For the eluent (HCl/ethanol 1:1, *v*/v) concentration, it was observed that better results are obtained for high levels of HCl (standardized effect of 59.95), which shows that for lower concentration, there are an incomplete elution of Cd^{2+} from micro-column. Therefore, the elution concentration was set to 1.0 mol L^{-1} HCl in ethanol as the best condition. The third most significant factor was the adsorbent mass, which also showed a positive significant effect in the response, clearly demonstrating a better response whenever adsorbent mass gets closer to 80.0 mg. From this result, it can still be noticed that the increase in adsorbent mass enhances the amount of Cd^{2+} adsorbent on the HIIP, but does not influence in the elution profile (transient signal). Therefore, this finding led us to select 80.0 mg as the best condition. Higher levels were not investigated to avoid leakages and overpressure in the micro-column. Regarding buffer solution concentration, it was observed a negative influence in the response (standardized effect of −8.521) when higher level was employed. Such result suggests that high ionic concentration of buffer solution (0.1 mol L^{-1}) makes the diffusion of Cd^{2+} towards the surface of adsorbent difficult or the ions from solution may compete with Cd^{2+} for binding sites. According to influence of pH and buffer solution concentration in the preconcentration system, the optimum values of these factors were determined from a Doehlert matrix carried out in triplicate at central point (Table 5). The analytical response to be optimized was absorbance (peak height) and the experiments were performed by loading 10.0 mL of Cd^{2+} solution at concentration of 5.0 μg L^{-1}, flow rate of 5.0 mL min^{-1}, adsorbent mass of 80.0 mg and HCl 1.0 mol L^{-1} in ethanol (1:1, v/v).

Table 5
Doehlert matrix used in the optimization of the sample pH and buffer solution concentration.

Assays	BSC (mol L^{-1})		pH		Absorbance (peak height)
1	0	(0.051)	0	(7.0)	0.468
1	0	(0.051)	0	(7.0)	0.475
1	0	(0.051)	0	(7.0)	0.472
2	1.0	(0.1)	0	(7.0)	0.303
3	0.5	(0.0755)	0.866	(9.0)	0.344
4	−1.0	(0.002)	0	(7.0)	0.345
5	−0.5	(0.0265)	−0.866	(5.0)	0.140
6	0.5	(0.0755)	−0.866	(5.0)	0.124
7	−0.5	(0.0265)	0.866	(9.0)	0.351

The first number represents the Doehlert matrix coded values, whereas the values between parentheses stand for the real values.

The Doehlert matrix was modeled by a second-order model represented by following equation:

$$Abs = -0.0487pH^2 + 0.730pH - 61.50BSC^2 + 5.58BSC + 0.0459pHxBSC \quad (9)$$

The validity of second-order model was checked from analysis of variance (ANOVA). The $MS_{lack\ of\ fit}/MS_{erro\ pure}$ ratio of 3.136 was lower than the tabled critical value $F_{1,2}$ of 18.513, indicating the absence of lack of fit of model. After validation process, the optimum values of pH (7.56) and buffer solution concentration (0.048 mol L^{-1}) were determined from the surface response (Fig. 8) derived from second-order model.

3.9. Influence of potentially interfering ions on the preconcentration system of Cd^{2+}

Bearing in mind that proposed preconcentration method has been developed for its application in samples with different matrices, the influence of possible interferences from concomitant metal ions was evaluated in the determination of Cd^{2+}. The interference was evaluated individually when potentially interfering ions promote a change in the cadmium signal alone at about ±10%. In this sense, the determination of 5.0 μg L^{-1} Cd^{2+} was not affected by addition of Ca^{2+} or Mg^{2+} up to 500.0 μg L^{-1}, while measurements of Cd^{2+} in the presence of Zn^{2+}, Pb^{2+}, Cu^{2+}, Fe^{2+}, Hg^{2+} or Co^{2+} at 250.0 μg L^{-1} did not present interferences. From the achieved results, it can be seen that cations have no obvious influence on the preconcentration system of Cd^{2+}.

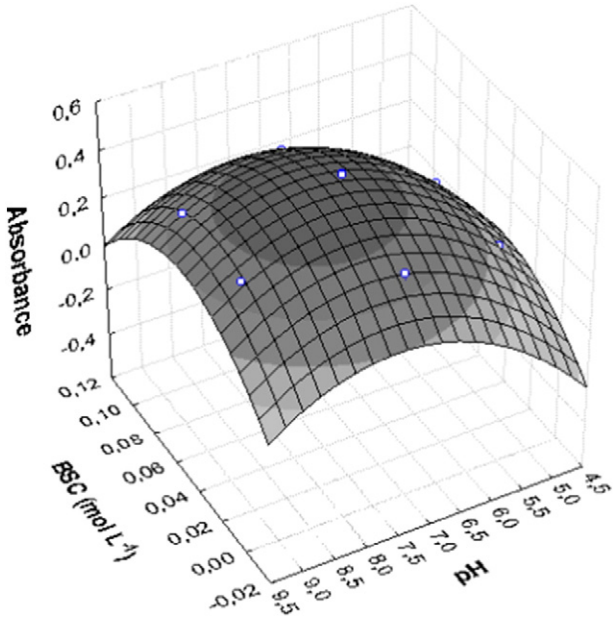

Fig. 8. Response surface derived from Doehlert matrix and second-order model.

3.10. Analytical characteristics of preconcentration system of Cd^{2+}

The analytical characteristics were determined under optimized conditions. Analytical curve of method was varied from 0.5 up to 7.0 μg L^{-1}, resulting in the following linear equation:

$$\text{Abs} = 0.00767 + 0.0842\left[Cd^{2+}, \mu g\ L^{-1}\right]\ \left(R^2 = 0.998\right) \quad (10)$$

The sensitivity (Abs L. μg^{-1}) of this linear equation was compared to those values obtained from the linear relationship achieved by direct Cd^{2+} determination by TS-FF-AAS (Eq. (11)) and by direct aspiration of Cd^{2+} into the FAAS nebulizer (Eq. (12))

$$\text{Abs} = -0.00205 + 0.0061\ \left[Cd^{2+}, \mu g\ L^{-1}\right]\ \left(R^2 = 0.998\right) \quad (11)$$

$$\text{Abs} = 0.0004 + 0.0003\ \left[Cd^{2+}, \mu g\ L^{-1}\right]\ \left(R^2 = 0.999\right) \quad (12)$$

The ratio between the slopes of the linear Eqs. (10) and (11) gave a preconcentration factor of 14-fold, revealing the outstanding improvement in the sensitivity by implementing the preconcentration step. When the on-line coupling of preconcentration system with TS-FF-AAS was compared to sensitivity of FAAS, a preconcentration factor of 280-fold was achieved, thus demonstrating the great usefulness of developed preconcentration method in terms of sensitivity. The limits of detection (LOD = 30 ng L^{-1}) and quantification (LOQ = 100 ng L^{-1}) were based on 3Std/S and 10std/S, respectively, where Std is the standard deviation of 10 measurements of blank solution and S is the sensitivity of linear equation [52]. The consumption index (CI) of proposed method, defined as the sample volume (10.0 mL) employed in the preconcentration step divided by the preconcentration factor (14), was found to be 0.71 mL. The sample throughput of proposed method was 15 h^{-1}, considering the sample loading of 10.0 mL at a flow rate of 5.0 mL min^{-1}. The intra-day precision of method was found to be 3.9 and 0.6% (relative standard deviation) for 10 consecutive measurements of standard solutions of Cd^{2+} at 0.7 and 6.5 μg L^{-1}, respectively. The inter-day precision (two different days) for the same concentrations of Cd^{2+} was found to be 4.4 and 2.4%.

In order to confirm the synergic effect of dual functional monomers for creating imprinting cavities with the features of organic-inorganic hybrid polymer, the sensitivity of proposed method has been compared to those obtained by using the non-imprinted hybrid polymer (HNIP) (Eq. (13)), organic (OIIP) (Eq. (14)) and inorganic (IIIP) (Eq. (15)).

$$\text{Abs} = 0.00668 + 0.0255\ \left[Cd^{2+}, \mu g\ L^{-1}\right]\ \left(R^2 = 0.989\right) \quad (13)$$

$$\text{Abs} = 0.00573 + 0.0398\ \left[Cd^{2+}, \mu g\ L^{-1}\right]\ \left(R^2 = 0.992\right) \quad (14)$$

$$\text{Abs} = 0.00172 + 0.0435\ \left[Cd^{2+}, \mu g\ L^{-1}\right]\ \left(R^2 = 0.991\right) \quad (15)$$

By comparing the slopes of these linear equations with that achieved in Eq. (10), it can be clearly observed that HIIP provided the highest sensitivity for Cd^{2+} determination among the four adsorbents used. Moreover, the stability of HIIP can be considered highly satisfactory because all the optimization processes, the interference studies and application of method in real samples were performed by using only one micro-column. Thus, the potential regeneration of the micro-column was estimated to be 211 times, but more preconcentration-elution cycles may still be carried out without decrease in the adsorptive performance of material.

Some analytical characteristics of proposed method have been compared to previous published preconcentration method for Cd^{2+} determination by TS-FF-AAS (Table 6). The comparison suggests advantages of proposed method using the novel hybrid ion imprinted polymer, such as absence of toxic chelating agent in the flow preconcentration method, lower limit of detection as well as the obvious advantages of on-line method, which is very fast when compared to precipitation and cloud point extraction. The use of grape bagasse as adsorbent provided similar analytical characteristics with respect to our study and low sampling consumption. However, the biosorbent presents worst selectivity and stability (80 cycles).

3.11. Application of preconcentration system of Cd^{2+} in real samples and accuracy

Aiming at demonstrating the feasibility of developed method, different matrices were analyzed and subjected to recovery tests after spiking procedure with known amount of Cd^{2+} (Tables 7 and 8). As one can see, the high recovery values (94.3–106.0%) indicate the high potential of developed method for free-interference determination of Cd^{2+} from drinking (mineral, tap), environmental water sample (lake water), as well as from urine and cigarettes samples. Besides the high recovery

Table 6
Comparative data regarding the analytical features of preconcentration methods for the Cd^{2+} determination by TS-FF-AAS.

Preconcentration method or adsorbent	Chelating agent/precipitant agent	Preconcentration modality	Volume (mL)	PF	LOD (ng L^{-1})	References
Precipitation	NH_3	On-line	4.0	34	40	[53]
Cloud point	APDC	Off-line	10.0	13	40	[54]
Fullerene	APDC	On-line	1.5	11	100	[55]
Grape Bagasse	–	On-line	4.0	34	30	[56]
Polyurethane foam	DDTP	On-line	2.0	5	120	[57]
New hybrid ion imprinted polymer (HIIP)	–	On-line	10.0	14	30	This study

V – volume of sample, PF – preconcentration factor, LD – limit of detection, APDC – ammonium pyrrolidinedithiocarbamate; DDTP – ammonium O,O-diethyl dithiophosphate.

Table 7
Application of developed method in water samples, urine and evaluation of recovery tests.

Samples	Cd^{2+} (μg L^{-1})		
	Amount added	Amount found[a]	Recovery (%)
Mineral water 1	0	<LOD	–
	1.0	1.06 ± 0.02	106
	3.0	3.03 ± 0.05	101
Mineral water 2	0	<LOD	–
	1.0	1.01 ± 0.07	102
	3.0	2.95 ± 0.04	98
Tap water	0	<LOD	–
	1.0	1.06 ± 0.03	102
	3.0	3.06 ± 0.02	101
Lake water	0	<LOD	–
	1.0	1.04 ± 0.02	104
	3.0	3.04 ± 0.06	101
Urine 1	0	<LOD	–
	3.0	2.89 ± 0.07	96
Urine 2	0	<LOD	–
	3.0	2.85 ± 0.10	95

<LOD – below of limit of detection.
[a] Results are expressed as mean value ± standard deviation based on three replicates ($n = 3$).

values, which attest the accuracy of method for real samples; we have also evaluated the accuracy from analysis of certified reference material DOLT-4 (fish liver). The obtained value of 23.9 ± 0.6 mg kg^{-1} ($n = 3$) was statistically equal to certified value of 24.3 ± 0.8 mg kg^{-1} (*Student t-test* at confidence interval of 95%).

4. Conclusion

The highlight of the present study herein demonstrated for the first time relies upon on the successful use of an ion-selective bifunctional hybrid imprinted adsorbent with attractive properties towards the adsorption and preconcentration of Cd^{2+}. The bifunctional hybrid imprinted polymer (HIIP), synthesized with 4-vinylpyridine (4-VP) and 3-mercaptopropyltrimethoxysilane as functional groups containing binding sites capable to interact with Cd^{2+}, not only exhibited a better selectivity and adsorption capacity than the non-imprinted hybrid polymer (HNIP), but also a higher adsorption of Cd^{2+} when compared to the organic (OIIP) and inorganic (IIIP) imprinted polymers. Overall, the characterization by FT-IR, SEM, X-ray diffraction and TGA allowed us to obtain insight into the formation of organic and inorganic phases with more details. Kinetic, adsorption isotherm and thermodynamic studies were successfully applied in the adsorption studies, which allowed us to clearly identify the presence of binding sites with different energies responsible for the adsorption of Cd^{2+}, and differentiate the adsorption nature that takes place in the HIIP and HNIP. In regard to analytical performance of on-line preconcentration method for Cd^{2+} coupled to TS-FF-AAS, this work proves that taking advantage of the imprinting effect created in the bifunctional hybrid imprinted adsorbent, a highly selective, sensitive and simple method for Cd^{2+} determination can be obtained and applied with precision and accuracy in a wide range of different samples. The advance in the preparation of ion imprinted polymer by exploiting bifunctional hybrid materials here reported may be extended to the development of new preconcentration systems by using imprinting technologies with highly enhanced performance.

Table 8
Determination of Cd^{2+} in cigarette sample using the developed method.

Sample	Cd^{2+} (μg g^{-1})		
	Amount added	Amount found[a]	Recovery (%)
Cigarette	0	1.10 ± 0.05	–
	1.20	2.17 ± 0.06	94
	2.40	3.33 ± 0.08	95

[a] Results are expressed as mean value ± standard deviation based on three replicates ($n = 3$).

Acknowledgements

The authors would like to thank the Conselho Nacional de Desenvolvimento Científico e Tecnológico (CNPq) (Grant Nos. 481669/2013-2, 305552/2013-9, 472670/2012-3), Coordenação de Aperfeiçoamento de Pessoal de Nível Superior (CAPES) (25/2014), Fundação Araucária do Paraná (163/2014), Laboratório de Espectroscopia da Central de Multiusuário da PROPPG, SANEPAR (09/2014), SETI do Paraná, ESPEC-UEL and Instituto Nacional de Ciência e Tecnologia de Bioanalítica (INCT) (Grant No. 573672/2008-3) for their financial support and fellowships.

References

[1] H. Nishide, J. Deguchi, E. Tsuchida, Selective adsorption of metal ions on crosslinked poly(vinylpyridine) resin prepared with a metal ion as a template, Chem. Lett. 5 (1976) 169–174.
[2] H. Nishide, E. Tsuchida, Selective adsorption of metal ions on poly(4-vinylpyridine) resins in which the ligand chain is immobilized by cross-linking, Makromol. Chem. 177 (1976) 2295–2310.
[3] L.D. Marestoni, M.D.P.T. Sotomayor, M.G. Segatelli, L.R. Sartori, C.R.T. Tarley, Ion imprinted polymers: fundamentals, preparation strategies and applications in analytical chemistry, Quim Nova 36 (2013) 1194–1207.
[4] T.P. Rao, S. Daniel, J.M. Gladis, Tailored materials for preconcentration or separation of metals by ion-imprinted polymers for solid-phase extraction (IIP-SPE), Trends Anal. Chem. 23 (2004) 28–35.
[5] Y. Zhai, Y. Liu, X. Chang, X. Ruan, J. Liu, Metal ion-small molecule complex imprinted polymer [membranes: preparation and separation characteristics], React. Funct. Polym. 68 (2008) 284–291.
[6] T. Alizadeh, M. Rashedi, Synthesis of nano-sized arsenic-imprinted polymer and its use as As^{3+} selective ionophore in a potentiometric membrane electrode: part 1, Anal. Chim. Acta 843 (2014) 7–17.
[7] F.M. de Oliveira, A.C. Gonçalves Jr., D.C. Dragunski, M.G. Segatelli, C.R.T. Tarley, Application of Ni(II)-imprinted cross-linked poly(methacrylic acid) synthesized through double-imprinting method for the on-line preconcentration of Ni(II) ions in aqueous media, Int. J. Environ. Anal. Chem. 94 (2014) 1–11.
[8] M.C. Barciela-Alonso, V. Plata-Garcia, A. Rouco-López, A. Moreda-Piñeiro, P. Bermejo-Barrera, Ionic imprinted polymer based solid phase extraction for cadmium and lead pre-concentration/determination in seafood, Microchem. J. 114 (2014) 106–110.
[9] J. Fasihi, M. Shamsipur, A. Khanchi, M. Mohani, K. Ashtari, Imprinted polymer grafted from silica particles for on-line trace enrichment and ICP OES determination of uranyl ion, Microchem. J. 126 (2016) 316–321.
[10] J. Liu, X. Yang, X. Cheng, Y. Peng, H. Chen, Synthesis and application of ion-imprinted polymer particles for solid-phase extraction and determination of trace scandium by ICP-MS in different matrices, Anal. Methods 5 (2013) 1811–1817.
[11] H.R. Rajabi, M. Shamsipur, M.M. Zahedi, M. Roushani, On-line flow injection solid phase extraction using imprinted polymeric nanobeads for the preconcentration and determination of mercury ions, Chem. Eng. J. 259 (2015) 330–337.
[12] T.P. Rao, R. Kala, S. Daniel, Metal ion-imprinted polymers—novel materials for selective recognition of inorganics, Anal. Chim. Acta 578 (2006) 105–116.
[13] C. Branger, W. Meouche, A. Margaillan, Recent advances on ion-imprinted polymers, React. Funct. Polym. 73 (2013) 859–875.
[14] C.R.T. Tarley, M.D.P.T. Sotomayor, L.T. Kubota, Polímeros biomiméticos em Química Analítica. Parte 1: preparo e aplicações de MIP ("Molecularly Imprinted Polymers") em técnicas de extração e separação, Quim. Nova 28 (2005) 1076–1086.
[15] M. Shamsipur, J. Fasihi, K. Ashari, Grafting of ion-imprinted polymers on the surface of silica gel particles through covalently surface-bound initiators: a selective sorbent for uranyl ion, Anal. Chem. 79 (2007) 7116–7123.
[16] T.C. de Ávila, M.G. Segatelli, L.A. Beijo, C.R.T. Tarley, Employ of silica gel organically modified and ionically imprinted for selective on-line preconcentration of copper ions, Quim Nova 33 (2010) 301–308.
[17] W. Behbahani, A. Bagheri, M. Taghizadeh, M. Salarian, O. Sadeghi, L. Adlnasab, K. Jalali, Synthesis and characterisation of nano structure lead (II) ion-imprinted polymer as a new sorbent for selective extraction and preconcentration of ultra trace amounts of lead ions from vegetables, rice, and fish samples, Food Chem. 138 (2013) 2050–2056.
[18] T.O. Germiniano, M.Z. Corazza, M.G. Segatelli, E.S. Ribeiro, M.J.S. Yabe, E. Galunin, C.R.T. Tarley, Synthesis of novel copper ion-selective material based on hierarchically imprinted cross-linked poly(acrylamide-*co*-ethylene glycol dimethacrylate), React. Funct. Polym. 82 (2014) 72–80.
[19] X. Cai, J. Li, Z. Zhang, F. Yang, R. Dong, L. Chen, Novel Pb^{2+} ion imprinted polymers based on ionic interaction via synergy of dual functional monomers for selective solid-phase extraction of Pb^{2+} in water samples, ACS Appl. Mater. Interfaces 6 (2014) 305–313.
[20] C.R.T. Tarley, F.N. Andrade, F.M. de Oliveira, M.Z. Corazza, L.F. de Azevedo, M.G. Segatelli, Synthesis and application of imprinted polyvinylimidazole-silica hybrid

copolymer for Pb^{2+} determination by flow-injection thermospray flame furnace atomic absorption spectrometry, Anal. Chim. Acta 703 (2011) 145–151.
[21] N.T. Hoai, D.-K. Yoo, D. Kim, Batch and column separation characteristics of copper-imprinted porous polymer micro-beads synthesized by a direct imprinting method, J. Hazard. Mater. 173 (2010) 462–467.
[22] C.R.T. Tarley, F.N. Andrade, H. Santana, D.A.M. Zaia, L.A. Beijo, M.G. Segatelli, Ion-imprinted polyvinylimidazole-silica hybrid copolymer for selective extraction of Pb(II): characterization and metal adsorption kinetic and thermodynamic studies, React. Funct. Polym. 72 (2012) 83–91.
[23] M.X. Liu, Y. Sun, S. Na, F. Yan, Selective adsorption of lead(II) from aqueous solution by ion-imprinted PEI-functionalized silica sorbent: studies on equilibrium isotherm, kinetics, and thermodynamics, Desalin. Water Treat. 57 (2016) 3270–3282.
[24] Y.-K. Lv, L.-M. Wang, L. Yang, C.-X. Zhao, H.-W. Sun, Synthesis and application of molecularly imprinted poly(methacrylic acid)–silica hybrid composite material for selective solid-phase extraction and high-performance liquid chromatography determination of oxytetracycline residues in milk, J. Chromatogr. 1227 (2012) 48–53.
[25] C.R.T. Tarley, N.C. Farias, G.F. Lima, F.M. de Oliveira, R. Bonfílio, D.C. Dragunski, D.N. Clausen, M.G. Segatelli, Crosslinked poly (4-vinylpyridine-ethylene glycol dimethacrylate) used for preconcentration of Cd(II) and its determination by flow injection flame atomic absorption spectrometry, J. AOAC 97 (2014) 605–611.
[26] M.Z. Corazza, B.F. Somera, M.G. Segatelli, C.R.T. Tarley, Grafting 3-mercaptopropyl trimethoxysilane on multi-walled carbon nanotubes surface for improving on-line cadmium(II) preconcentration from water samples, J. Hazard. Mater. 243 (2012) 326–333.
[27] International Agency for Research on Cancer (IARC), Proceedings of the meeting of the IARC working group on beryllium, cadmium, mercury and exposures in the glass manufacturing industry, Scand. J. Work Environ. Health 19 (1993) 360.
[28] M. Andac, R. Say, A. Denizli, Molecular recognition based cadmium removal from human plasma, J. Chromatogr. B 811 (457) (2004) 119–126.
[29] W. Plazinski, W. Rudzinski, A. Plazinska, Theoretical models of sorption kinetics including a surface reaction mechanism: a review, Adv. Colloid Interf. Sci. 152 (2009) 2–13.
[30] I.A. Sengil, M. Özacar, H. Tükmenler, Kinetic and isotherm studies of Cu(II) biosorption onto valonia tannin resin, J. Hazard. Mater. 162 (2009) 1046–1052.
[31] M.M.C. Lopez, M.C.C. Perez, M.S.D. Garcia, J.M.L. Vilariño, M.V.G. Rodriguez, L.F.B. Losada, Preparation, evaluation and characterization of quercetin-molecularly imprinted polymer for preconcentration and clean-up of catechins, Anal. Chim. Acta 721 (2012) 68–78.
[32] A. Wong, F.M. de Oliveira, C.T.T. Tarley, M.D.P.T. Sotomayor, Study on the cross-linked molecularly imprinted poly(methacrylic acid) and poly(acrylic acid) towards selective adsorption of diuron, React. Funct. Polym. 100 (2016) 26–36.
[33] R. Say, A. Ersöz, H. Türk, A. Denizli, Selective separation and preconcentration of cyanide by a column packed with cyanide-imprinted polymeric microbeads, Sep. Purif. Technol. 40 (2004) 9–14.
[34] F.M. de Oliveira, M.G. Segatelli, C.R.T. Tarley, Hybrid molecularly imprinted poly(methacrylic acid-TRIM)-silica chemically modified with (3-glycidyloxypropyl)trimethoxysilane for the extraction of folic acid in aqueous medium, Mater. Sci. Eng. C 59 (2016) 643–651.
[35] K.M. Diniz, M.G. Segatelli, C.R.T. Tarley, Synthesis and adsorption studies of novel hybrid mesoporous copolymer functionalized with protoporphyrin for batch and on-line solid-phase extraction of Cd^{2+} ions, React. Funct. Polym. 73 (2013) 838–846.
[36] S. Chen, D. Du, J. Huang, A. Zhang, H. Tu, A. Zhang, Rational design and application of molecularly imprinted sol–gel polymer for the electrochemically selective and sensitive determination of Sudan, Talanta 84 (2011) 451–456.
[37] F.M. de Oliveira, M.G. Segatelli, C.R.T. Tarley, Evaluation of a new water-compatible hybrid molecularly imprinted polymer combined with restricted access for the selective recognition of folic acid in binding assays, J. Appl. Polym. Sci. 133 (2016) 43463–43473.
[38] N. Zhang, B. Hu, Cadmium (II) imprinted 3-mercaptopropyltrimethoxysilane coated stir bar for selective extraction of trace cadmium from environmental water samples followed by inductively coupled plasma mass spectrometry detection, Anal. Chim. Acta 723 (2012) 54–60.
[39] D.D. Maksin, S.O. Kljajevic, M.B. Dolic, J.P. Markovic, B.M. Ekmescic, A.E. Onjia, A. Nastasovic, Kinetic modeling of heavy metal sorption by vinyl pyridine based copolymer, Hem. Ind. 66 (2012) 795–804.
[40] B. Gao, D. Kong, Y. Zhang, Preparation and catalytic activity of P4VP–Cu(II) complex supported on silica gel, J. Mol. Catal. A Chem. 286 (2008) 143–148.
[41] L.R. Nacano, M.G. Segatelli, C.R.T. Tarley, Elective sorbent enrichment of nickel ions from aqueous solutions using a hierarchically hybrid organic-inorganic polymer based on double imprinting concept, J. Braz. Chem. Soc. 21 (2010) 419–430.
[42] H. Ma, T. Shi, Q. Son, Synthesis and characterization of novel PVA/SiO_2-TiO_2 hybrid fibers, Fibers 2 (2014) 275–284.
[43] L.M. Costa, E.S. Ribeiro, M.G. Segatelli, D.R. Do Nascimento, F.M. De Oliveira, C.R.T. Tarley, Adsorption studies of Cd(II) onto Al_2O_3/Nb_2O_5 mixed oxide dispersed on silica matrix and its on-line preconcentration and determination by flame atomic absorption spectrometry, Spectrochim. Acta B 66 (2011) 329–337.
[44] I.A.W. Tan, B.H. Hammed, A.L. Ahmad, Equilibrium and kinetic studies on basic dye adsorption by oil palm fibre activated carbon, Chem. Eng. J. 127 (2007) 111–119.
[45] K.C. Bedin, A.C. Martins, A.L. Cazetta, O. Pezoti, V.C. Almeida, KOH-activated carbon prepared from sucrose spherical carbon: adsorption equilibrium, kinetic and thermodynamic studies for methylene blue removal, Chem. Eng. J. 286 (2016) 476–484.
[46] R.G. Pearson, Hard and soft acids and bases, J. Am. Chem. Soc. 85 (1963) 3533–3539.
[47] A.M. Awwad, N.M. Salem, Kinetics and thermodynamics of Cd(II) biosorption onto loquat (*Eriobotrya japonica*) leaves, J. Saudi Chem. Soc. 18 (2014) 486–493.
[48] A.Z. Aroguz, Kinetics and thermodynamics of adsorption of azinphosmethyl from aqueous solution onto pyrolyzed (at 600 °C) ocean peat moss (*Sphagnum* sp.), J. Hazard. Mater. 135 (2006) 100–105.
[49] C.R.T. Tarley, M.Z. Corazza, B.F. Somera, M.G. Segatelli, Preparation of new ion-selective cross-linked poly(vinylimidazole-*co*-ethylene glycol dimethacrylate) using a double-imprinting process for the preconcentration of Pb^{2+} ions, J. Colloid Interface Sci. 450 (2015) 254–263.
[50] M.A. Al-Anber, Thermodynamics approach in the sorption of heavy metals, in: J.C. Moreno-Pirajan (Ed.), Thermodynamics – Interaction Studies – Solids, Liquids and Gases, InTech, New York 2011, pp. 737–764.
[51] C.R.T. Tarley, G. Silveira, W.N.L. dos Santos, G.D. Matos, E.G.P. da Silva, M.A. Bezerra, M. Miró, S.L.C. Ferreira, Chemometric tools in electroanalytical chemistry: methods for optimization based on factorial design and response surface methodology, Microchem. J. 92 (2009) 58–67.
[52] G.L. Long, J.D. Winefordner, Limit of detection, Anal. Chem. 55 (1983) (A712-&).
[53] X. Wen, P. Wu, K. Xu, J. Wang, X. Hou, On-line precipitation–dissolution in knotted reactor for thermospray flame furnace AAS for determination of ultratrace cadmium, Microchem. J. 91 92009) 193–196.
[54] P. Wu, Y. Zhang, Y. Lv, X. Hou, Cloud point extraction–thermospray flame quartz furnace atomic absorption spectrometry for determination of ultratrace cadmium in water and urine, Spectrochim. Acta 61 (2006) 1310–1314.
[55] M.G. Pereira, E.R. Pereira-Filho, M.A.Z. Arruda, Determination of cadmium and lead at low levels by using preconcentration at fullerene coupled to thermospray flame furnace atomic absorption spectrometry, Spectrochim. Acta 59 (2004) 515–521.
[56] G.D. Matos, M.A.Z. Arruda, Online preconcentration/determination of cadmium using grape bagasse in a flow system coupled to thermospray flame furnace atomic absorption spectrometry, Spectrosc. Lett. 39 (2006) 755–768.
[57] C.R.T. Tarley, M.A.Z. Arruda, A sensitive method for cadmium determination using an on-line polyurethane foam preconcentration system and thermospray flame furnace atomic absorption spectrometry, Anal. Sci. 20 (2004) 961–966.